



# Combining Neural Networks and Data Assimilation to enhance the spatial impact of Argo floats in the Copernicus Mediterranean biogeochemical model

Carolina Amadio<sup>1</sup>, Anna Teruzzi<sup>1</sup>, Gloria Pietropoli<sup>1,2</sup>, Luca Manzoni<sup>2</sup>, Gianluca Coidessa<sup>1</sup>, and Gianpiero Cossarini<sup>1</sup>

<sup>1</sup>Istituto Nazionale di Oceanografia e di Geofisica Sperimentale – OGS, Trieste, 34100, Italy

<sup>2</sup>Dipartimento di Matematica e Geoscienze, Università degli Studi di Trieste H2bis Building, Via Alfonso Valerio 12/1, 34127 Trieste, Italy;

**Correspondence:** C. Amadio (camadio@ogs.it)

**Abstract.** Biogeochemical-Argo (BGC-Argo) float profiles provide substantial information for key vertical biogeochemical dynamics and successfully integrated in biogeochemical models via data assimilation approaches. Although results on the BGC-Argo assimilation are encouraging, data scarcity remains a limitation for their effective use in operational oceanography.

To address availability gaps in the BGC-Argo profiles, an Observing System Experiment (OSE), that combines Neural Network (NN) and Data Assimilation (DA), has been performed here. NN was used to reconstruct nitrate profiles starting from oxygen profiles and associated Argo variables (pressure, temperature, salinity), while a variational data assimilation scheme (3DVarBio) has been upgraded to integrate BGC-Argo and reconstructed observations in the Copernicus Mediterranean operational forecast system (MedBFM). To ensure high quality of oxygen data, a post-deployment quality control method has been developed with the aim of detecting and eventually correcting potential sensors drift.

5 The Mediterranean OSE features three different setups: a control run without assimilation; a multivariate run with assimilation of BGC-Argo chlorophyll, nitrate, and oxygen; and a multivariate run that also assimilates reconstructed observations.

The general improvement of skill performance metrics demonstrated the feasibility in integrating new variables (oxygen and reconstructed nitrate). Major benefits have been observed in reproducing specific BGC process-based dynamics such as the nitracline dynamics, primary production and oxygen vertical dynamics.

15 The assimilation of BGC-Argo nitrate corrects a generally positive bias of the model in most of the Mediterranean areas, and the addition of reconstructed profiles makes the corrections even stronger. The impact of enlarged nitrate assimilation propagates to ecosystem processes (e.g., primary production) at basin wide scale, demonstrating the importance of BGC-profiles in complementing satellite ocean colour assimilation.

## 1 Introduction

20 The Array for Real-time Geostrophic Oceanography (Argo) programme appears to be one of the better examples of countries and human resource capacities in working together to provide global data coverage (Miloslavich et al., 2019) that supports the



investigation of the present (analysis), future (forecast) and past years (reanalysis) ocean state conditions. In the last 10 years, the increase of in-situ observations from autonomous platforms (Johnson et al. 2013 and Johnson and Claustre 2016) has opened up new perspectives for biogeochemical oceanographers. Indeed, BGC-Argo (biogeochemical Argo, 2023) has yielded  
25 new insights in describing the interior of the global ocean (Le Traon, 2013) and key processes such as the deep chlorophyll maximum (Mignot et al. 2014, Barbieux et al. 2019, D'ortenzio et al. 2020, Ricour et al. 2021, and Barbieux et al. 2022), oxygen and (Capet et al., 2016), nutrients vertical fluxes (Taillandier et al. 2020 and Wang et al. 2021b) and carbon exports (Dall'Olmo and Mork 2014 and Wang and Fennel 2023).

Among the BGC sensors, oxygen (O<sub>2</sub>) is currently the most common measured variable, with approximately 270,000 pro-  
30 files worldwide until now, which is double that of suspended particles and chlorophyll and more than four times those of nitrate, downwelling irradiance, and pH (<https://biogeochemical-argo.org>). Currently, the Global Data Assembly Centres (GDACs, e.g., Coriolis, NOAA) distributes oxygen data in Real Time (RT) Adjusted (AM) and Delayed Mode (DM). The quality of AM data is controlled within 24 hours using internationally agreed and automatic quality-control procedures performed at the surface, along the entire vertical profiles and along the trajectory (Thierry and Bittig, 2021). DM data are generally distributed  
35 a few months later (nearly six months) in more rigorous form (Li et al., 2020).

Major efforts have been devoted to improve the long-term reliability and accuracy of autonomous O<sub>2</sub> measurements (Sauzède et al., 2017). As described in Takeshita et al. (2013) and in Maurer et al. (2021), raw oxygen data from floats can have errors of up to 20% in terms of oxygen saturation (at the surface) due to sensor drift during storage out of the water. By improving the accuracy up to 5-10%, 1st-order correction methods can correct storage drift by multiplying the oxygen concentrations  
40 with a gain factor derived from a reference dataset (Johnson et al., 2015). Additionally, oxygen measurements are calibrated using values of saturation at the surface (in water for the older ones and in air for floats with new sensors, Bushinsky et al. 2016). Despite correction and calibration progress, Maurer et al. (2021) and Bushinsky et al. (2016) found a drift in about 25% (mean drift -0.07% per year) and 70% (mean -0.12% per year) of analyzed floats, respectively. Positive and negative values of drift were found in Johnson and Claustre (2016) and Bittig et al. (2018b). Therefore, the development and dissemination  
45 of a post-deployment quality control (QC) method has been encouraged to avoid spurious results (Wang et al., 2020) and to distinguish between ocean signals or trends (e.g., deoxygenation) and potential optode drift.

The combination of in-situ observations and numerical models represents a promising approach to exploit the BGC-Argo potentialities. Indeed, BGC-Argo data are used for several BGC modelling tasks such as: (i) model tuning (Wang et al., 2020), (ii) validation ( Terzić et al. 2019, Salon et al. 2019 and Wang et al. 2021a), and (iii) assessment of the BGC ocean state and variability through data assimilation (DA) (Cossarini et al. 2019 and Teruzzi et al. 2021 d'Ortenzio et al. 2021). DA underpins decades of progress in ocean prediction (Geer, 2021) by increasing the type and number of observational datasets and associated uncertainty into a prediction model, and solving problems connected to uneven distribution and scarcity of the observations (Buizza et al., 2022).

Given their capacity to approximate continuous functions (Hornik et al., 1989), NN algorithms match specific DA tasks such  
55 as bias correction (Kumar et al. 2015 and Zhou et al. 2021), cross calibration (Lary et al., 2018), reformulation of observation operators (Storto et al., 2021) and new product creation or dataset reconstruction (Lary et al., 2018). As an example, ocean

color (OC) datasets were employed to test Multi-Layer Perceptrons (MLP, namely the most common NN) by retrieving past and long-term BGC time-series (Martinez et al. 2020a, Martinez et al. 2020b, Roussillon et al. 2023). Moreover, in Sauzède et al. (2016), MLP serves to infer vertical BGC distribution from OC. High performance in predicting biogeochemical states (e.g., oxygen) from physical profiling floats measurements were achieved in Stanev et al. (2022) for the Black Sea.

In Sauzède et al. (2017), an MLP-NN is used to approximate nutrient concentration and carbonate system from physical and oxygen profiles, and the updated version of Bittig et al. (2018c) allows refining the previous work with the so-called Canyon-b NN method. A configuration to adapt global Canyon-b NN in the Mediterranean Sea region is developed by Fourier et al. (2020). A further update of the application of the MLP method in the Mediterranean Sea is provided in Pietropolli et al. (2023), by achieving a lower error in the predictions through a larger training dataset, a hyperparameter refinement and a two-step quality control of the input data.

In the context of operational oceanography, the biogeochemical modelling component of the Copernicus Marine Service for the Mediterranean Sea (MedBFM) provides analysis, short term forecast (Salon et al., 2019) and long term reanalysis (Cossarini et al., 2021), including the assimilation of satellites Ocean Colour (OC) and BGC-Argo observations (Salon et al., 2019).

The variational assimilation scheme, 3DVarBio, of MedBFM has evolved over time by including a greater number of observation types and variables. Starting from the first release (Teruzzi et al., 2014), the assimilation has progressively included coastal OC observations (Teruzzi et al., 2018), chlorophyll and nitrate profiles from BGC-Argo (Cossarini et al. 2019 and Teruzzi et al. 2021 respectively). Given the growing availability of O<sub>2</sub> from BGC-Argo, in this paper we propose an additional upgrade of the MedBFM to include BGC-Argo oxygen assimilation, with a novel post-deployment quality control, and the integration of NN reconstructed profiles in the assimilation scheme.

The constant evolution of the observation networks and assimilation capacities requires an updated understanding of the impact of observation on the numerical model result (Gasparin et al., 2019). This can be achieved by using the numerical assimilative models in Observing System Experiments (OSEs) where the impact of existing observations on the model performance is assessed (Le Traon et al., 2019).

In this paper, our OSE experiment, that combines data assimilation and neural network in a sequential modular approach (hereafter NN-MLP-MED), aims at quantifying how Argo and BGC-Argo networks can be exploited. Spatial and temporal impacts of the OSE have been evaluated using classic and new skill performance metrics in three two-year (2017-2018) numerical experiments performed using the MedBFM coupled with the 3DVarBio: a control run (HIND) without assimilation; a multivariate run (DAfl) with assimilation of BGC-Argo chlorophyll, nitrate, and oxygen; and a multivariate run that also assimilates in-situ observations and reconstructed ones (DAnn).

Given its particular characteristics and the high density of BGC-Argo profiles, the Mediterranean Sea represents an ideal site for OSE experiments to evaluate the potentiality of the BGC-profiles assimilation. The Mediterranean Sea is an anti-estuarine semi-enclosed sea characterized by specific physical and biogeochemical dynamics (Pinardi et al., 2015), with a complex horizontal circulation consisting of mesoscale and sub-basins scale gyre structures, transitional cyclonic and anticyclonic gyres and eddies, influenced by bathymetric features interconnected by currents and jets (Oddo et al., 2009). Despite its relatively limited



extent in the mid-latitude temperate zone, the Mediterranean Sea has a considerable BGC variability that can be roughly approximated in an oligotrophic West-East gradient with low nutrient availability at the surface, insufficient to sustain significant phytoplankton biomass (Siokou-Frangou et al. 2010 and Marañón et al. 2021) and a deeper nitracline in the east (>120m) with respect to the west (<100m). Additionally, chlorophyll has a particular seasonal cycle with pronounced winter/early spring surface blooms only in the western part and a few locations in the eastern part. During summer, a deep chlorophyll maximum follows the stratified and oligotrophic conditions at increasing depth moving eastward (>100m at East and <100m in the West) (Teruzzi et al., 2021). Dissolved oxygen has a subsurface maximum at about 50m, with higher values in the west (partly due to the dependence of oxygen solubility on temperature). Noticeable differences are observed in the intermediate layers where the oxygen minimum ranges between 300 (west) and 1000 m (east) (Di Biagio et al., 2022).

The paper is organized as follows. After a brief presentation of the OSE approach, each component and the experimental setup are described in detail (Section 2). In the following section (Section 3), we describe the results of the novel NN-MLP-MED and the assimilation simulations by using different skill metrics to assess model capability in reproducing the main biogeochemical seasonal dynamics. A discussion of some key issues involved in the NN and DA is provided in Section 4, then the paper closes with some final remarks (Section 5).

## 2 Methods

A novel combined Neural Network (NN-MLP-MED) and Data Assimilation (3DVarBio) approach is included in the Mediterranean MedBFM model system to integrate BGC-Argo and reconstructed profiles into biogeochemical simulations of the Mediterranean Sea.

Our OSE experiment is based on a sequential modular approach (Buizza et al., 2022) consisting of a post-deployment quality control method of O<sub>2</sub>, hereafter QC O<sub>2</sub> procedure, a trained multi-layer perceptron NN (Pietropoli et al., 2023) and a data assimilation scheme (the 3DVarBio variational scheme of MedBFM, Figure 1).

The input of the first two modules, QC O<sub>2</sub> and NN-MLP-MED are the BGC-Argo and Argo datasets, while the final 3DVarBio module also takes the enhanced datasets as input: quality checked O<sub>2</sub> (qcO<sub>2</sub>) and reconstructed nitrate (recNO<sub>3</sub>, Figure 1).

In the following sections, the novel modules of the MedBFM system (i.e., the QC O<sub>2</sub> procedure and the NN-MLP-MED scheme) and the dataset (BGC-Argo and reconstructed datasets) are described together with the revised 3D-VarBio.

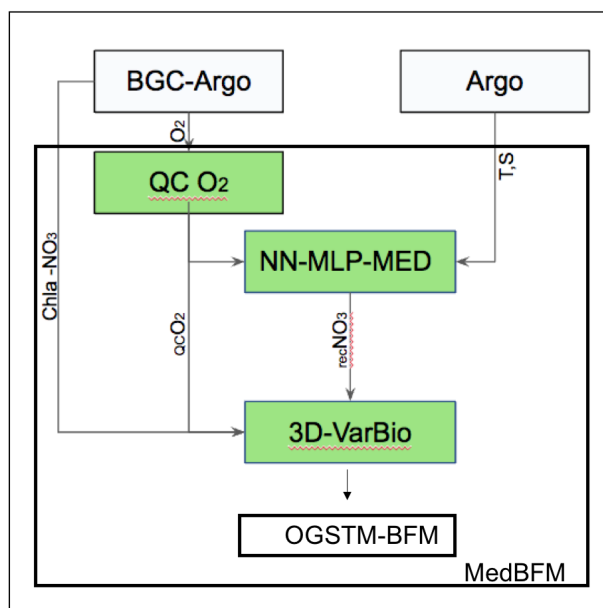


**Figure 1.** Flowchart of the NN-MLP-MED and DA approach. In green boxes: the modules. In plain boxes: the datasets. Arrows refers to Argo (temperature and salinity) and BGC Argo profiles of chlorophyll (Chla), oxygen (qcO<sub>2</sub>) nitrate (NO<sub>3</sub>) and reconstructed nitrate (recNO<sub>3</sub>)

## 2.1 The regional model for the Mediterranean Sea, MedBFM

The MedBFM consists of the OGS transport model (OGSTM) based on the OPA 8.1 system (Foujols et al., 2000) and updated according to the Lazzari et al. (2012) and Lazzari et al. (2016) versions, the BFM, Biogeochemical Flux Model described in Vichi et al. (2007a) and Vichi et al. (2007b), and the 3DVarBio variational assimilation scheme as in Teruzzi et al. (2014) and Teruzzi et al. (2018).

OGSTM solves advection, diffusion, sinking terms and the free surface and variable volume-layer effects on the transport of tracers (Salon et al., 2019), and it is forced by the output (current, T, S and sea surface height) of the NEMO3.2 model. OGSTM and NEMO3.2 share the same bathymetry and z\* grid configuration, open boundary and river conditions (Coppini et al., 2023).

The Biogeochemical Flux Model, BFM, is a biomass and functional group based marine ecosystem model. BFM solves governing equations for nine living-organic state variables (diatoms, autotrophic nanoflagellates, picophytoplankton, dinoflagellates, carnivorous and omnivorous mesozooplankton, bacteria, heterotrophic nanoflagellates, and microzooplankton, macronutrients (nitrate, phosphate, silicate and ammonium) and labile, semi-labile, and refractory organic matter and oxygen. In addition, the BFM includes a carbonate system model (Cossarini et al. 2015a and Canu et al. 2015).



## 2.2 3DVarBio data assimilation scheme

Based on 3DVarBio (Teruzzi et al. 2014, Teruzzi et al. 2018, Cossarini et al. 2019 and Teruzzi et al. 2021), the assimilation scheme adopted in the present work integrates oxygen, chlorophyll and nitrate to update all the assimilated variables as well as all the phytoplankton biomasses and phosphate.

The 3DVarBio is a variational data assimilation scheme (Teruzzi et al., 2014) based on the minimization of a cost function ( $J$ ) which relies on the misfit between the model background ( $x_b$ ) and the observations ( $y$ ) weighted with the respective error covariance matrices ( $B$  and  $R$ ) as follows:

$$J(x_a) = (x_a - x_b)^T B^{-1} (x_a - x_b) + (y - H(x_b))^T R^{-1} (y - H(x_b)) \quad (1)$$

Here, the observation operator ( $H$ ) maps the values of model background state in the observation space. Following Dobricic et al. (2006), the background error covariance matrix,  $B$ , is factorised as  $B=VV^T$  with  $V=V_V V_H V_B$ . The  $V$  operators describe different aspects of the error covariances: the vertical error covariance ( $V_V$ ), the horizontal error covariance ( $V_H$ ), and the state variable error covariance ( $V_B$ ).  $V_V$  is defined by a set of reconstructed profiles evaluated by means of an Empirical Orthogonal Function (EOF) decomposition applied to a validated multi-annual 1998-2015 run (Teruzzi et al., 2018). EOFs are computed for 12 months and 30 coastal and open sea sub-regions in order to account for the variability of biogeochemical anomaly fields.  $V_H$  is built using a Gaussian filter whose correlation radius modulates the smoothing intensity. A non-uniform and direction-dependent correlation radius has been implemented as in Cossarini et al. (2019).  $V_B$  operator consists of prescribed monthly and sub-region varying covariances among the biogeochemical variables (e.g., nitrate to phosphate). Specifically, for the assimilation of chlorophyll, the  $V_B$  operator includes a balance scheme that maintains the ratio among the phytoplankton groups and preserves the physiological status of the phytoplankton cells (i.e., preserve optimal values for the internal chlorophyll, carbon and nutrients quota). The operators  $V_V$  and  $V_B$  of the 3DVarBio have been updated for the assimilation of oxygen.  $V_V$  involved the calculation of specific EOF profiles for oxygen including a localization function to avoid spurious assimilation in the deepest part of the water column.  $V_B$  included only a new direct relation for oxygen (i.e., oxygen assimilation update only the oxygen itself), given that it has been shown that it barely affects other variables (Skakala et al., 2021).

Assimilated observations are composed by the QC BGC-Argo listed in Table 1. Oxygen and nitrate profiles in the 0-600 m layer are used in the assimilation, while chlorophyll is assimilated in the 0-200 m layer.

The observation error covariance matrix  $R$  is diagonal with a monthly varying error in chlorophyll (Cossarini et al., 2019). In nitrate and reconstructed nitrate profiles, the observation error is constant in time and increases along the vertical with a constant values of  $0.25 \text{ mmol m}^{-3}$  in the 0-450 meters layer (Mignot et al., 2019) and linearly increasing of up to  $0.35 \text{ mmol m}^{-3}$  between 450-600m (nitrate maximum assimilation depth). Although the accuracy of the reconstruction of profiles is  $0.87 \text{ mmol m}^{-3}$  (Pietropoli et al., 2023), we decided to not use different values of error for the two nitrate subsets in order to show the highest potential impact of the OSE.

Observation error for oxygen is set to  $5 \text{ mmol m}^{-3}$  in the upper 200 meters of depth and gradually goes to  $20 \text{ mmol m}^{-3}$  in correspondence of the maximum assimilation depth.



### 165 2.3 The neural network architecture and the reconstructed nitrate dataset

The NN-MLP-MED (Pietropolli et al., 2023) is the evolution of previous MLP architectures developed to predict low-sampled variables (e.g., nutrients) starting from high-sampled ones (e.g., temperature) (Sauzède et al. 2017 , Bittig et al. 2018c and Fourier et al. 2020)

170 The NN-MLP-MED presents some novel elements with respect to the mentioned methods (and in particular with respect to Canyon-Med in Fourier et al. 2020), which lead to improved results. Firstly, the input dataset includes a larger sample size and broader coverage of the Mediterranean Sea region. Secondly, the quality of the input dataset benefits from a two-step quality check process, removing noisy and unreliable samples. The neural network architecture was also modified to enhance prediction performance by incorporating nonlinear functions, adjusting neuron count, and optimizing the training algorithm. The error of reconstructed nitrate, obtained by using the EMODnet as validation dataset, was  $0.5 \text{ mmol m}^{-3}$  (Pietropolli et al., 175 2023)

In our OSE experiment, the trained NN-MLP-MED is used to reconstruct nitrate profiles from temperature and salinity (Argo), oxygen (BGC-Argo) and float date, latitude and longitude. The reconstruction also includes a vertical smoothing (running mean of 5-10 m window) and an adjustment to the 600 m climatology derived from EMODnet (Salon et al., 2019).

180 The input nitrate dataset for assimilation is made up of 938 BGC-Argo profiles and 2146 reconstructed nitrate profiles (Table 1). The reconstructed nitrate profiles are located 61% in the western and 39% in the eastern Mediterranean Sea, thus providing a larger and more homogeneous spatial coverage as shown in Figures 2.

### 2.4 BGC-Argo data and post-deployment oxygen quality control

BGC-Argo profiles available between the 2017-2018 period were downloaded from Coriolis GDAC (last visit on July 2022). Adjusted and delayed mode data were selected for oxygen and chlorophyll, while exclusively DM data were considered for 185 nitrate.

Table 1 reports the total number of BGC-Argo profiles, characterized by a significant number of oxygen and chlorophyll data against the relative paucity of nitrate. Figure 2 shows the spatial distribution of the BGC profiles of chlorophyll and nitrate, while oxygen coverage can be approximated by merging nitrate and reconstructed nitrate profiles locations. Despite the lack of data in specific sub-basins (Alboran, South Western Ionian and Northern Adriatic Seas), all the three BGC variables have a 190 fairly homogeneous spatial coverage between the western and eastern Mediterranean Sea.

Since oxygen sensors may drift and lose accuracy over time, the accurate determination of dissolved oxygen is typically more challenging and requires some form of correction (Johnson et al., 2015). Expressed in % per year, the loss of accuracy is observed over the time, particularly 12 months after the deployment (<https://www.euro-argo.eu>). Deep ocean drift is considered as a proxy for oxygen sensor drift because of the lack of seasonal and annual signals for oxygen at depth (Takeshita et al., 2013).

195 Here, the optode sensor in-situ drift is evaluated through non parametric tests (RANSAC and Theil Sen) at two different depths (600 and 800 meters). Tests are applied when the life of a float is longer than 1 year.

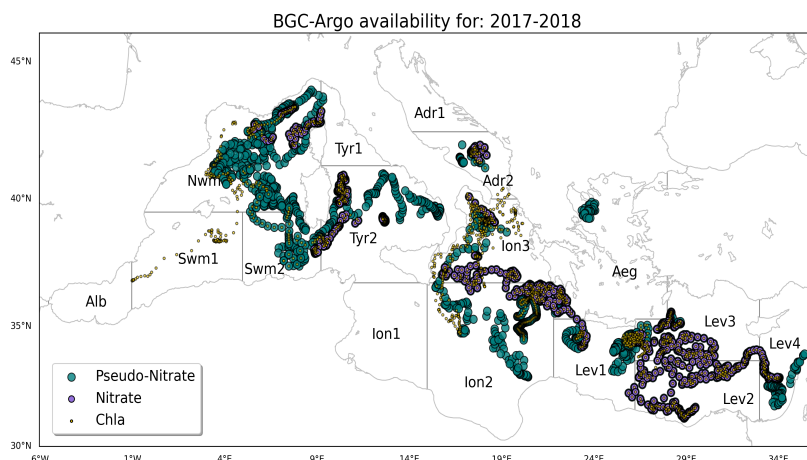


**Figure 2.** BGC-profiles of chlorophyll-a (red), Nitrate in-situ (orange) and reconstructed Nitrate (grey) assimilated in Mediterranean Sea (2017-2018). Subdivision of the Mediterranean domain in sub-basins used for the validation. According to data availability and to ensure consistency and robustness of the metrics, different subsets of the sub-basins or some combinations among them can be used for the different metrics: lev=lev1+lev2+lev3+lev4; ion=ion1+ion2+ion3; tyr=tyr1+tyr2; adr=adr1+adr2; swm=swm1+swm2.

The RANSAC and Theil Sen methods split the oxygen dataset into a set of inliers and outliers and drift is estimated only using inliers, avoiding possible biases due to the outliers (Dang et al. 2008 and Fischler and Bolles 1981).

The presence of a drift is established when all four drift estimates agree in sign and their average value is greater than 1 mmol m<sup>-3</sup> y. This threshold was chosen on the basis of results in Bittig et al. (2018b).

When detected, the suspicious drift is removed from the oxygen profiles by setting the computed drift values (i.e., the average of the four estimates) at 600 meters and linearly interpolating toward the surface, where drift is set equal to zero. Indeed, it can be assumed that O<sub>2</sub> values at surface are already fixed by the GDACs (Thierry and Bittig, 2021).

## 2.5 Design of numerical experiments

Three numerical experiments were performed to analyze the impact of different assimilation setups. Simulated period is 1.1.2017-31.12.2018, and the MedBFM setup mostly corresponds to the standard adopted in the Mediterranean Analysis and Forecast biogeochemical system of the Marine Copernicus Service. Set up includes open boundary conditions in the Atlantic, climatological input of nutrients, carbon and alkalinity for 39 rivers and the Dardanelles Straits; and initial conditions from EMODnet dataset (Details are provided in Salon et al. 2019 ).

Our experimental setup differs from the standard one for the physical forcing, which are from Mediterranean Copernicus reanalysis (Escudier et al., 2021), and the initial conditions of oxygen which are retrieved from BGC-Argo float climatology computed after QC O<sub>2</sub> procedure (described in section 2.4).





Test Case	Chl	O2	NO3	Updated variables
HIND	–	–	–	–
DAfl	1773	1924	938	phyto biomass, NO3 , O2 and PO4
DAnn	1773	1924	2146	phyto biomass, NO3 , O2 and PO4

**Table 1.** Summary of the numerical experiments and assimilated BGC-profiles

The three simulations, which share the same setup except for the assimilated datasets, are: (1) control run without assimilation (HIND); (2) assimilation of BGC-Argo chlorophyll, nitrate and oxygen and (DAfl) (3) assimilation of additional reconstructed nitrate profiles used to enhance the DAfl assimilative set up (DAnn).

Before integrating data in the 3D-VarBio, the same pre-assimilation assessments described in Teruzzi et al. (2021) were applied for chlorophyll. Nitrate profiles are rejected if concentration at the surface is higher than  $3 \text{ mmol m}^{-3}$ . Finally, oxygen exclusion is evaluated on the basis of the difference with the oxygen saturation values, using a threshold of  $10 \text{ mmol m}^{-3}$  and comparing oxygen data at 600m with respect to a reference dataset using a threshold of 2 times the standard deviation of the reference dataset. For the reference dataset, we used the EMODnet2018\_int data collection that integrates the in-situ aggregated EMODnet data (Buga et al., 2018) and the datasets listed in Lazzari et al. (2016) and Cossarini et al. (2015b). The EMODnet2018\_int dataset is available for 16 sub-basins (see Figure 2) in the Mediterranean Sea.

During the data assimilation, profiles can be excluded when model-observation misfit is higher than given thresholds. For chlorophyll the threshold is set  $2 \text{ mg m}^{-3}$  and it must be found in at least 5 vertical levels in the 0-50m layer. For nitrate, the misfit thresholds are set to 2 and  $3 \text{ mmol m}^{-3}$  in 0-50 m and 250-600m layers, respectively. Exceeding misfit has to be found in at least 5 vertical levels. Oxygen profiles are discarded by defining misfit thresholds of 30 and  $50 \text{ mmol m}^{-3}$  in at least 5 vertical levels in the 0-150m and 150-600m layers respectively.

### 3 Results

#### 3.1 The oxygen post-deployment quality check method

The post deployment oxygen QC method allowed to automatically correcting in-situ sensor drifts.

Of the 40 floats available in the 2017-2018 period, the drift analysis was applied to 16 floats, while 24 floats could not be analyzed due to the limited length of the timeseries.

Over the 16 floats, a significant drift was found in 13 of them: 4 were affected by a positive drift and 9 by a negative one. The remaining 3 floats had lower drift values than the prescribed threshold (Section 2.4).

The absolute average correction of the 13 floats is about  $4.3 \text{ mmol m}^{-3} \text{ y}$  performed at 600 meters of depth. This quantity is in line with the ranges expressed in terms of sensor drift percentage in Bittig et al. (2018a) (1-1.5%).



Figure 3 shows an example of the evolution of oxygen profiles of a quasi-stationary float (6902687) detected for a drift correction. In line with the conclusion reported in several works such as Bittig et al. (2018a) and Maurer et al. (2021), the presence of a drift, like the one detected by our protocol, may reveal the possible tendency of the oxygen sensor to slowly degrade over time. After 2 years, the bias due to the drift was approximately  $5 \text{ mmol m}^{-3}$  (1st December 2017 profiles in Figure 3.)

After removing of drift, the deep oxygen concentrations results to be closer to the EMODnet climatological data, allowing to include a higher number of profiles (example in Figure 3, green star) in the assimilated O<sub>2</sub> datasets (Figure 1).

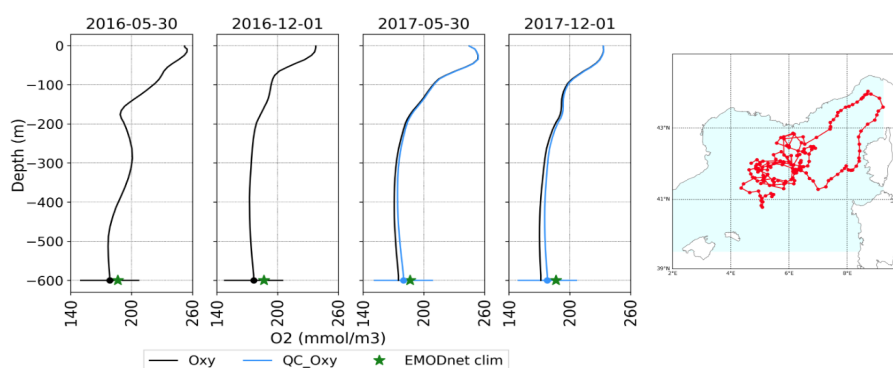


**Figure 3.** Original (black) and corrected (blue) oxygen profiles of float 6902687 on four selected dates. EMODnet climatology for nwm subbasin is reported (green star)

### 3.2 Validation using Satellite and BGC-Argo datasets

Skills performance of the simulations listed in Table 1 are evaluated by comparing model results with satellite OC chlorophyll and BGC-Argo profiles. While for the satellite comparison the model daily averages are considered, the model first guess (i.e. the model state before the assimilation) is used for metrics based on BGC-Argo.

Root Mean Square Error (RMSE) metric is evaluated in winter (from February to April, FMA) and summer (from June to August, JJA) to investigate the model's capacity to reproduce the specific bloom and stratification conditions in 16 Mediterranean Sea sub-basins or in an aggregated combination of them (Figure 2).

Satellite L3 products from Copernicus Marine Service catalogue were interpolated from 1 km to the model resolution and a composite weekly average was computed to ensure gap-free maps, as in Teruzzi et al. (2014).

The Winter RMSE with respect to OC chlorophyll in HIND spans between ca.  $0.09$  to  $0.21 \text{ mg m}^{-3}$  with a maximum in the Alboran Sea (Figure 4). The addition of multivariate DA (DAfl) has a positive impact with a reduction of surface errors of by 6.5% mainly observed in the eastern sub-basins. A further reduction of RMSE (up to 10%) with respect to HIND is then obtained with DAnn showing that enlarging the nitrate float network leads to improvements in reproducing surface phytoplankton dynamics. All the Mediterranean sub-basins show an RMSE reduction with the exception of alb, swm and nwm.



A generalized slight worsening in the assimilated runs can generally be observed during the summer stratification period. The RMSE with respect to OC chlorophyll, which increases in all sub-basins, is fairly similar in the two assimilation runs: about 6% and 7.5% in DAfl and DAnn, respectively. It should be noted that the RMSE values in summer are an order of magnitude lower than in winter, reflecting the seasonal chlorophyll variability in the Mediterranean Sea (i.e., the very low values of chlorophyll at the surface).

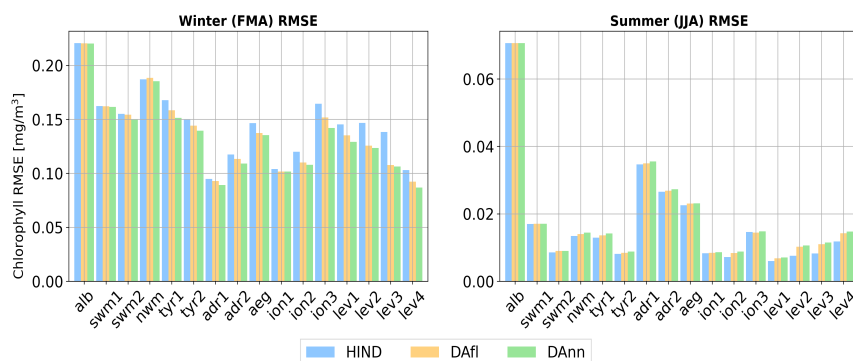


**Figure 4.** Seasonal chlorophyll RMSE: Winter bloom and Summer stratification seasons in the Mediterranean Sea sub-basins for the HIND run (light blue), the DAfl run (in orange) and the DAnn run (green)

The RMSE metrics based on BGC-Argo are computed for six selected aggregated macro-basins (Alboran, South West Mediterranean, North West Mediterranean, Tyrrhenian, Ionian and Levantine Seas) and in selected layers (0-10m, 10-30m, 30-60m, 60-100m, 100-150m, 150-300m and 300-600m) and are shown in Figure 5 for nitrate (top panel), chlorophyll (middle panel) and oxygen (bottom panel). It is worth recalling that only in-situ profiles are used in the validation (i.e., reconstructed NN profiles are used only for assimilation).

As expected, the assimilation of in-situ BGC-Argo considerably improves the quality of modelled nitrate with respect to the HIND run (Figure 5). Winter RMSE reduction goes from 40% (DAfl) to approximately 46%, when also reconstructed profiles are assimilated, while the reduction of summer RMSE increases from 59% in DAfl to 63% in DAnn. Maximum RMSE reduction of RMSE of DAnn with respect to DAfl is observed in nwm and tyr (winter) and in ion (summer). This impact can be directly ascribed to the increased number of reconstructed nitrate in these sub-basins and seasons where additional profiles generate more persistent corrections.

The advantages of assimilating chlorophyll profiles have been already shown in Teruzzi et al. (2021). Here, improvements related to chlorophyll assimilation can be observed in nwm, ion and lev in winter and at depth in tyr, ion and lev in summer (Figure 5 middle panel). Even if phytoplankton dynamics depend on nutrients dynamics, the positive impact of DAnn on nitrate RMSE does not transfer to the vertical chlorophyll statistics in the DAnn. This is mainly because the DAfl and DAnn simulations assimilate the same chlorophyll dataset, and the direct chlorophyll assimilation is more effective than the



280

dynamical model adjustment after nitrate and reconstructed nitrate assimilation in the areas close to the observed chlorophyll profiles.

Assimilating oxygen profiles enable reducing the model-BGC floats RMSE by about 30% during winter and summer. The correction involves the whole water columns with a maximum correction between 150-600m during winter in the west and along the entire profiles in the east (ion and lev) in both winter and summer. The addition of reconstructed profiles in the DAfl run does not significantly affect the quality of oxygen.

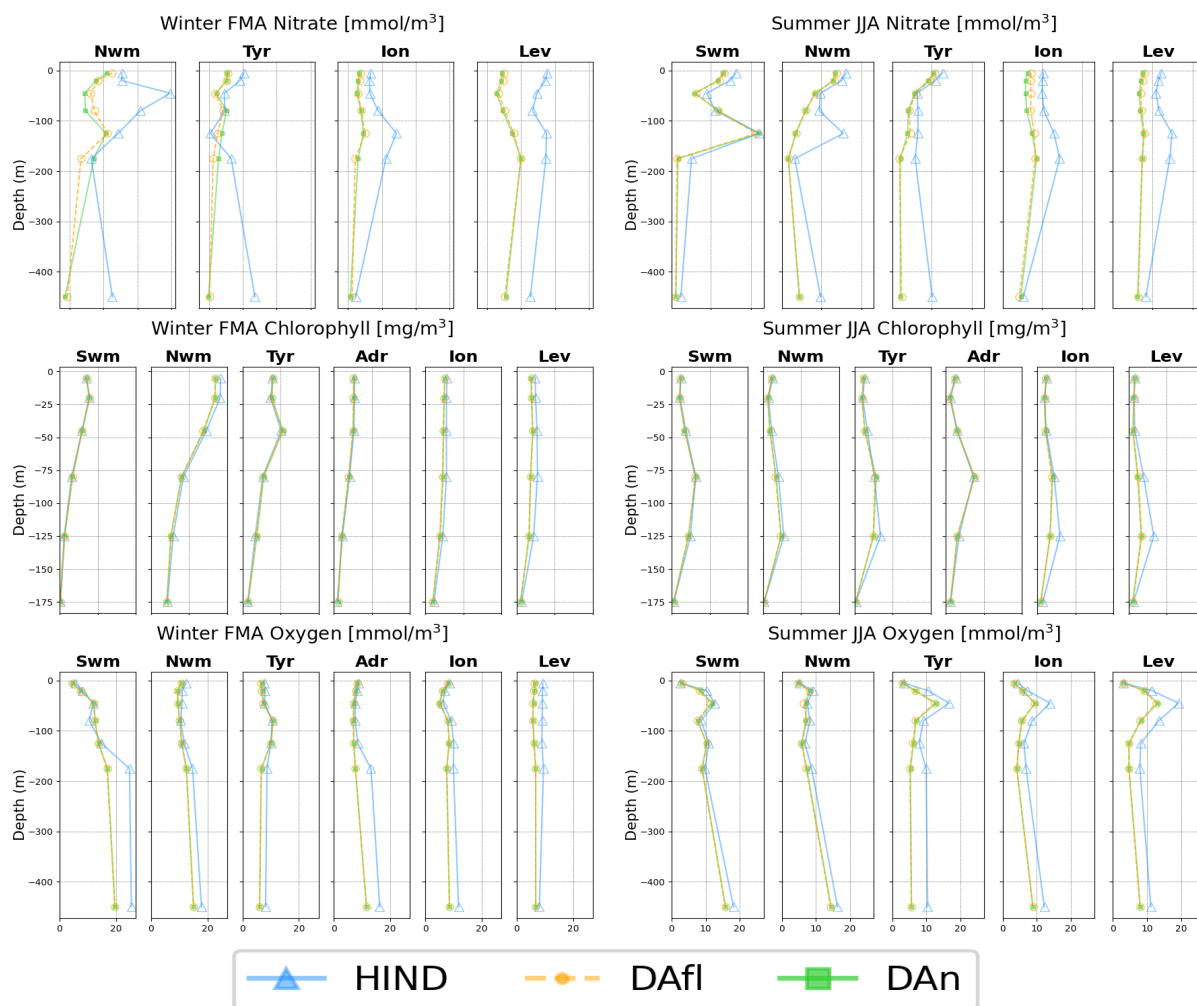


**Figure 5.** Seasonal Nitrate, Chlorophyll and Oxygen RMSE (top, middle, bottom): Bloom (left) and Stratification (right) seasons in the Mediterranean Sea aggregated sub-basins for the HIND run (pale blue), DAfl (orange) and DAn (green)



### 285 3.3 Integration of NN DA: the impact

#### 3.3.1 Impacts on biogeochemical vertical dynamics

As expected, the profile assimilation plays a major role in changing the vertical gradients of biogeochemical variables. Figures 6, 7, 8, and 9 show the impact of the assimilation in two sub-basins where the number of reconstructed profiles is high (Figure 2) and in the Mediterranean Sea (third column). The two sub-basins represent two different trophic conditions in the Mediterranean Sea. The North Western Mediterranean (nwm) has higher level of nutrient concentration and more intense surface bloom in winter (Siokou-Frangou et al. 2010 and Di Biagio et al. 2022). In summer, nwm has higher chlorophyll concentration at the deep chlorophyll maximum (DCM), shallow nitracline, and shallow subsurface oxygen maximum (SOM) (first column in Figures 6, 7, 8, and 9). On the contrary, more oligotrophic conditions and deeper nitracline and DCM are found in the eastern subbasin (ion2, second column of Figures 6, 7, 8, and 9). The assimilation of nitrate corrects a general positive bias of the model in all the Mediterranean areas (blue pattern in Figure 7). The addition of reconstructed profiles makes the corrections stronger. At the Mediterranean scale, the nitrate concentration below the nitracline decreases by 8% and 11% in DAfl and DAnn runs, respectively. Nitracline depth changes (i.e. deeper values) by DAfl assimilation by a few (nwm) and tens of meters (ion2). The deepening of the nitracline becomes more intense with the inclusion of reconstructed profiles (DAnn). The differences between the assimilation and reference runs accumulates over time and eventually reach a stationary phase in the second year in the sub-basins with a high number of BGC-Argo and reconstructed profiles, such as nwm and ion2. On the other hand, considering the whole Mediterranean Sea, which comprises some under-sampled areas (e.g., southern Ionian and southern western basin), the effect of corrections is still propagating after the two years (third column of Figure 7)

Very similar patterns are also observed in the Hovmöller diagrams of phosphate (Figure 8), which is an updated variable of the multivariate variational assimilation scheme through nitrate. In fact, the general negative corrections on phosphate fields are linked to the high positive values of the covariance matrix between nitrate and phosphate (Teruzzi et al., 2021)

As a consequence of both the direct assimilation of chlorophyll profiles and the dynamical model adjustment after nitrate assimilation, the main effects of DAfl are to slightly reduce the intensity of chlorophyll concentration in the DCM (e.g., variation smaller than 5% with respect to HIND simulation) and in adjusting the timing of the surface winter blooms (second row in Figure 6). Even if the chlorophyll validation (Figure 5) has not shown significant differences between DAfl and DAnn, the basin wide averages of DAnn display more intense corrections with respect to DAfl in terms of DCM depth and chlorophyll intensity and overall chlorophyll concentration (figure 6). Over the 0-200 layer of the entire Mediterranean Sea, the chlorophyll decreases with respects to HIND are 4% and 5% for DAfl and DAnn, respectively.

BGC-Argo oxygen profiles assimilation (DAfl, second row in Figure 9) provides positive or negative corrections depending on the observation-model bias which varies in time and space (e.g., mostly negative in nwm and mostly positive in ion2). On a Mediterranean basin-wide scale, the average correction is of 0.2% for the 0-200m layer. The addition of the nitrate reconstructed profiles does not alter the correction pattern with an average correction of 0.3%. The only noticeable difference between the two assimilation runs can be spotted in areas with a high density of reconstructed profiles during summer (e.g., nwm, first column in Figure 9). As observed in the nitrate and chlorophyll figures, the assimilation of reconstructed profiles



causes a decrease of the summer productivity in the DCM layer. Consequently, less oxygen is produced generating the negative  
 320 changes in the DCM layer in the bottom left panel of Figure 9. Because of the smaller amount of subsequent sinking organic  
 matter, less oxygen is consumed in remineralization processes in layers below the DCM in late summer and autumn, and  
 positive oxygen changes are generated, particularly during 2018.

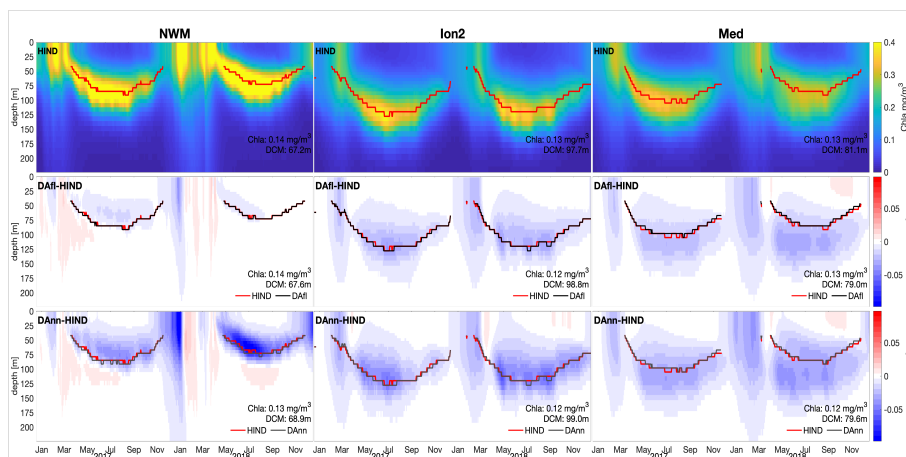


**Figure 6.** Hovmöller diagram of chlorophyll of hindcast simulation (first row) and differences between assimilation runs and hindcast (second and third rows) for 2 sub-basins (nwm and ion2) and the Mediterranean Sea (med). Evolution of the depth of nitracline for the three runs: red (hind) and black (DAfl and DAnn) lines. The averages of 0-200m concentration and of nitracline for the simulated period are reported.

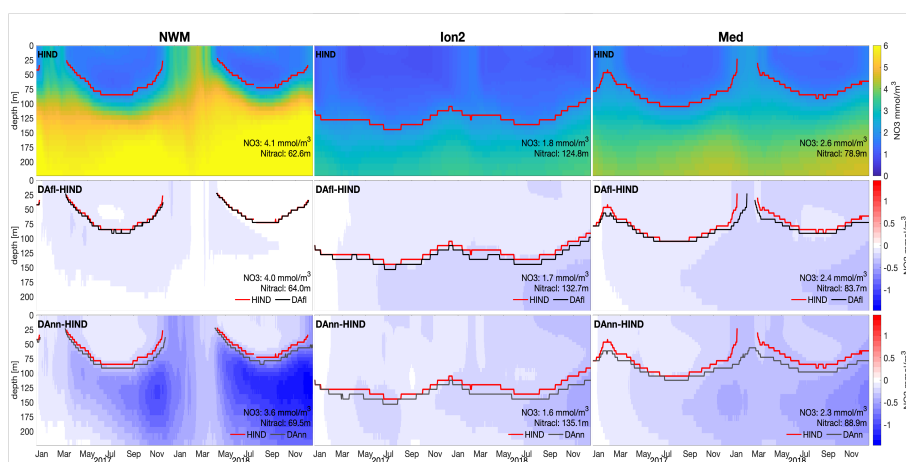


**Figure 7.** Hovmöller diagram of nitrate of hindcast simulation (first row) and differences between assimilation runs and hindcast (second and third rows) for 2 sub-basins (nwm and ion2) and the Mediterranean Sea (med). Evolution of the depth of nitracline for the three runs: red (hind) and black (DAfl and DAnn) lines. The averages of 0-200m concentration and of nitracline for the simulated period are reported.

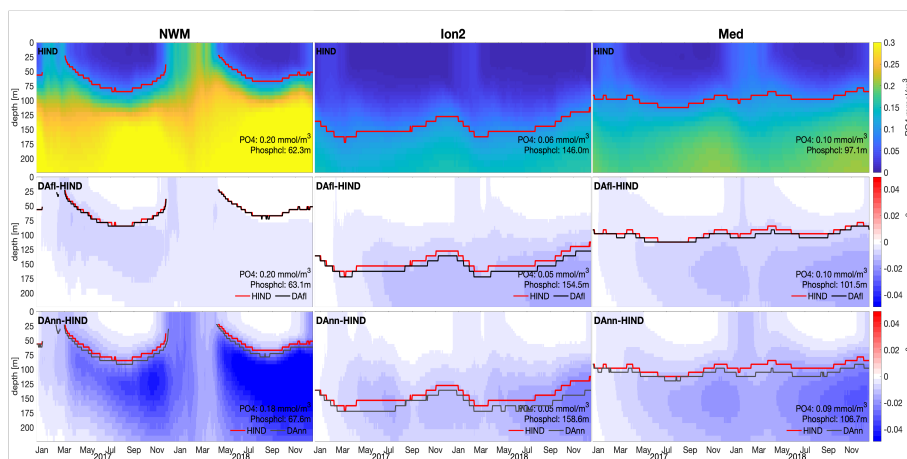


**Figure 8.** Hovmöller diagram of phosphate of hindcast simulation (first row) and differences between assimilation runs and hindcast (second and third rows) for 2 sub-basins (nwm and ion2) and the Mediterranean Sea (med). Evolution of the depth of phosphocline for the three runs: red (hind) and black (DAI and DAnn) lines. The averages of 0-200m concentration and of phosphocline for the simulated period are reported.

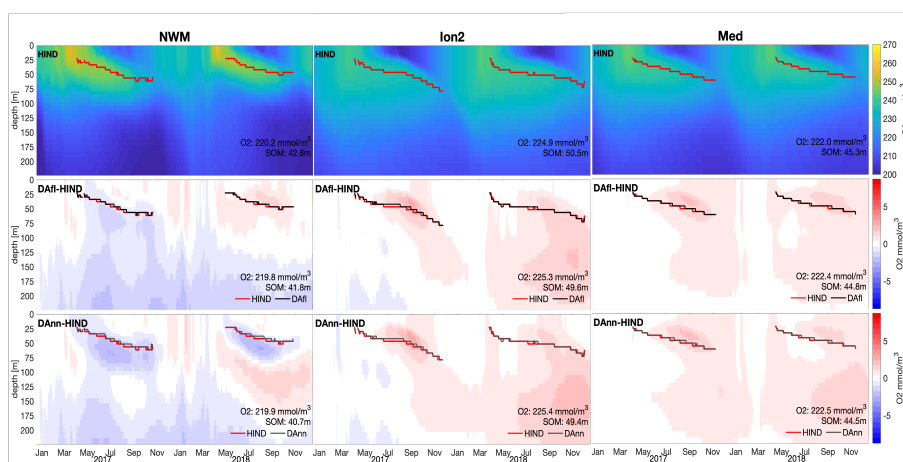


**Figure 9.** Hovmöller diagram of oxygen of hindcast simulation (first row) and differences between assimilation runs and hindcast (second and third rows) for 2 sub-basins (nwm and ion2) and the Mediterranean Sea (med). Evolution of the depth of subsurface oxygen maximum (SOM) for the three runs: red (hind) and black (DAI and DAnn) lines. The averages of 0-200m concentration and of SOM for the simulated period are reported.

### 3.3.2 Impact on ecosystem indicator

Net primary production (NPP) integrates phytoplankton growth and respiration processes which are at the basis of the marine trophic food web. Assimilation of chlorophyll and nitrate together with the updates of phosphate, directly and indirectly af-



fect primary production, since they impact phytoplankton biomass and nutrient availability. Thus, the comparison of primary production among the three simulations reveals how the assimilation impacts on a key indicator that integrates several marine ecosystem processes. Seasonal maps of net primary production integrated over the 0-200 m layer in the HIND, DAfl and DAnn simulations (Figure 10) confirm that the assimilation impact varies spatially and temporally. In the DAfl simulation, the largest differences in primary production with respect to the HIND simulation are located in the eastern Mediterranean with a decrease of nearly 10% in the Levantine sub-basins and in the Ionian Sea close to the Greek coast. Reductions are slightly larger in winter. In the western Mediterranean the impacts on primary production are negligible in both seasons with the only exception of a 5% reduction in winter in the Tyrrhenian Sea. Areas with changes on NPP corresponding to the areas with assimilation of float profiles that include nitrate. In the DAnn simulation, the impacts on primary production are more intense than in DAfl and the impacted areas are larger. In particular, primary production is decreased also in areas such as the western Mediterranean in summer (8%) and in the northwestern Mediterranean and in the Tyrrhenian Sea in winter (5%).

Moreover, a further reduction of NPP occurs in the Ionian Sea in both seasons. In general, the impact on primary production is greater where nitrate observations or nitrate reconstructed observations are assimilated, suggesting a dynamical bottom-up control of primary production. In fact, the weaker fertilization of the surface layer in DAnn, which occurs for both macronutrients after assimilation (Figure 7 and 8), appears to be the main cause of reduced NPP, outweighing the effects due to changes in phytoplankton biomass after chlorophyll assimilation.

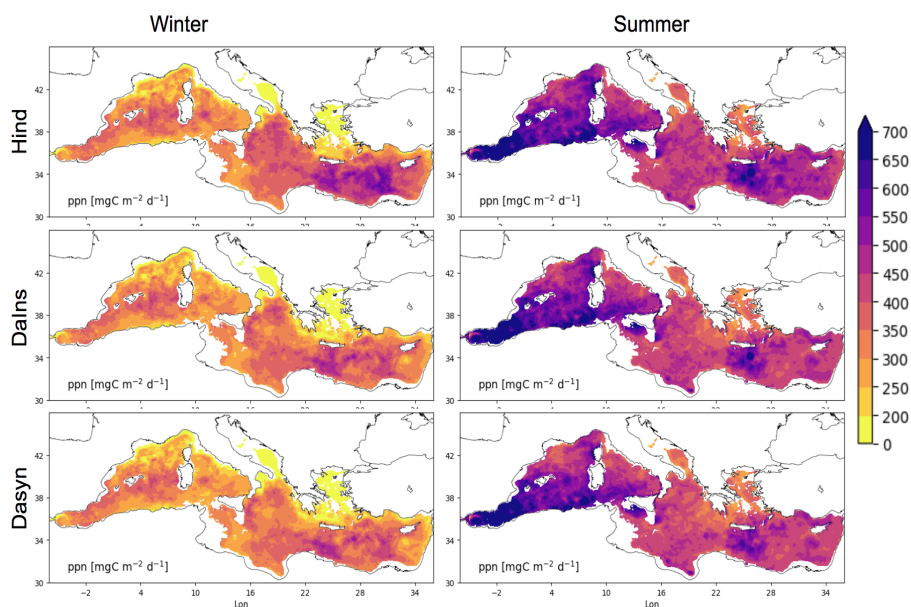


**Figure 10.** Maps of net winter (FMA) and summer (JJA) primary production [NPP, mgC m<sup>-2</sup> d<sup>-1</sup>] in the three runs: A. HIND B. DAfl C. DAnn. Seasonal averages are computed considering the period 2017-2018.





### 3.3.3 Impact on Argo Observing system design

Analyzing the departure of an assimilated simulation from a reference solution provides insights into the impact of the observing system design and several data impact indicators can be used (Ford 2021, Teruzzi et al. 2021 and Raicich and Rampazzo 2003). In this work, we adopt the impact indicator  $I_{ij}(t)$  described in Teruzzi et al. (2021), in order to quantify the integrated (0-300m) response of assimilating BGC Argo profiles with respect to the no assimilative run:

$$I_{ij}(t) = \frac{|Sim_{ij}(t) - HIND_{ij}(t)|_{300}}{(HIND_{300})_{mean}} \quad (2)$$

Here, HIND is here the reference, while Sim refers to one of the different DA set-ups.  $|Sim_{ij}(t) - HIND_{ij}(t)|$  is the absolute difference between simulations (for each day and grid point) while the subscript 300 represents the integral over the 0–300m. The indicator  $I_{ij}(t)$  quantifies how much an assimilated run deviates from the reference (HIND) simulation. Figures 11 and 12 show the nitrate and chlorophyll  $I_{ij}(t)$  95th percentile of the seasonal indicator in winter (left column) and in summer (right column) in the DAfl (first row) and DAnn (second row) simulations. The 95th percentile of the indicator shows that the BGC-Argo assimilation impacts (DAfl) both chlorophyll and nitrate.

In DAfl, the extent of nitrate  $I_{ij}(t)$  95th above 0.1 is 16.5% and 18.7% in winter and in summer respectively, with clear spatial distribution mapping the BGC-Argo density. The introduction of reconstructed profiles in DAnn make it possible to increase the nitrate impacted areas up to about 35% and 39% in winter and summer respectively. The DAnn impact increase is mainly localized in the western Mediterranean Seas and in the Ionian Sea, while the less evident impact in the Levantine, especially in summer, is mainly due to the low number of NN reconstructed nitrate in the area.

Chlorophyll impact maps (Figure 12) show that besides the direct impact of chlorophyll profiles assimilation, phytoplankton is also affected by the reconstructed nitrate assimilation. Compared to a threshold of 0.4, the impacted areas increase from 18.2% to 29.8% in winter and from 10.8% to 14.5 in summer in the DAfl and DAnn runs. These results suggest that the inclusion of reconstructed nitrate assimilation can potentially extend the impact to almost all the Mediterranean Sea, with the only exclusion of the marginal seas (Adriatic and Aegean) and the southern part of Ionian and Western sub-basins.

Oxygen impact maps (not shown) are very similar to nitrate DAnn maps and do not show differences between the two DA simulation, since the same QC oxygen dataset was assimilated in DAfl and DAnn.

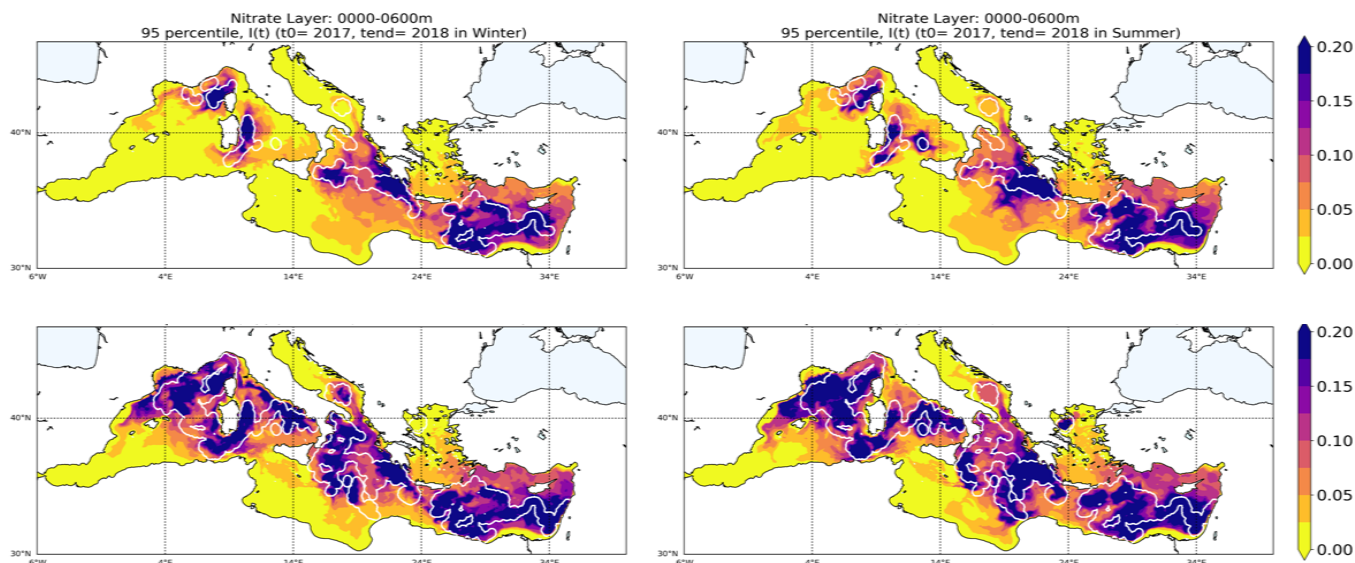


**Figure 11.** Maps of  $I_{ij}(t)$  95th percentiles for Nitrate in winter (left column) and summer (right column) in the DAfl (first row) and DAnn (second row); white contours identify the areas within three correlation radii from the float profiles

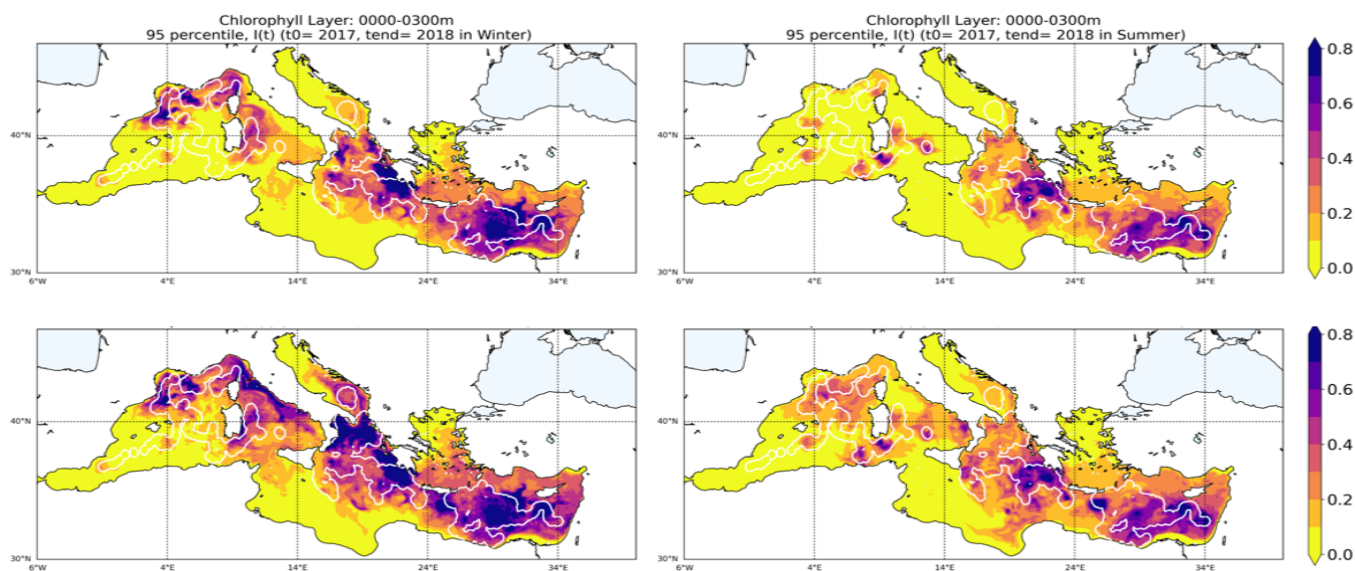


**Figure 12.** Maps of  $I_{ij}(t)$  95th percentiles for Chlorophyll in winter (left column) and summer (right column) in the DAfl (first row) and DAnn (second row); white contours identify the areas within three correlation radii from the float profiles



#### 4 Discussion

Our quality check procedure for oxygen drift detection and comparison with a reference dataset can successfully integrates the official QC BGC-Argo, making oxygen BGC-Argo a robust and valuable dataset for initial conditions, data assimilation, validation and new product reconstruction. Even if the distinction between real oxygen depletion signals and optode drift can  
370 remain problematic without in-situ high quality data, we believe that literature and prior knowledge can be used as a baseline for drift discrimination.

In particular, recent studies have revealed a decrease of oxygen concentrations in the Mediterranean Sea (Sisma-Ventura et al. 2021 and Di Biagio et al. 2022); such tendency has been defined as a multidecadal shifts (Coppola et al. 2018 and Mavropoulou et al. 2020) and also patchy deoxygenation (Mancini et al., 2023). One of the most evident signals is the early  
375 1990's East Mediterranean Transient (EMT) associated with the variations of thermohaline circulation, which has caused a strong interannual variability of oxygen (Sisma-Ventura et al., 2021). Based on this literature and considering the recent years, a threshold of  $1 \text{ mmol m}^{-3} \text{ y}$  at 600 and 800 meters appears a prudent limit for sensor drift discrimination from real long term signals.

Up to now, the oceanographer visual check is required to distinguishing ocean signals from sensor drift (Wang et al., 2020)  
380 and the debate on how to replace visual check to automatic statistical procedures is still open. Thus, our work can contribute by proposing a new tool to automatically handle deep ocean signal or optode drift issues.

The search of drift is based on a robust combination of several factors: (i) the float history has to be longer than 1 year, (ii) the calculation is done with two robust non-parametric trend methods and (iii) at two different depths (i.e. 600m and 800m) sampling different water masses that can have different long-term dynamics. Lastly, the sensor drift signal must be confirmed  
385 by the four results and has to be compared with typical basin-wide trend values reported by scientific literature (i.e., the choice of the threshold).

The method can be further developed by applying the oxygen drift analysis at some fixed isopycnals together with the one at constant isobaths. Thus, possible oxygen concentration changes due to floats moving across different water masses can be filtered out.

The assimilation of vertical profiles provides complementary information with respect to satellite ocean color assimilation  
390 (Cossarini et al. 2019 and Verdy and Mazloff 2017), which however is still the most commonly used in operational systems (Fennel et al., 2019). In fact, the effectiveness of the profiles assimilation, which has the capability to constrain vertical biogeochemical dynamics in subsurface layers (Kaufman et al. 2018, Teruzzi et al. 2021 and Wang et al. 2022), lies in the amount of available BGC-Argo data, that are generally insufficient to constrain a basin wide simulation. In Teruzzi et al. (2021), results of  
395 the impact indicator principally showed the efficiency of ocean color assimilation in constraining chlorophyll dynamics mostly during winter. In this work, important impacts are also observed in summer for all variables, as a consequence of the increased number of assimilated profiles.

In fact, through the integration of NN and DA, the number of nitrate profiles ingested can significantly increase, with a density of more than 30 profiles every ten days over a basin of  $2.5\text{M km}^2$ . Indeed, as shown in the results, Argo and BGC-Argo



400 oxygen sensors can potentially support a density of biogeochemical profiles up to 1 in each  $2.5^\circ \times 2.5^\circ$  box every 10 days. This means that seasonal sub-basins scale dynamics (e.g., bloom or stratification) can effectively be constrained while, up to now, mesoscale dynamics can probably be exclusively locally studied (d'Ortenzio et al., 2021). Apart from an increase in the numbers of floats, improvements in the simulation of mesoscale dynamics can be achieved by redefining horizontal covariance errors in the data assimilation scheme. Indeed, benefits of non-uniform correlation radius in the horizontal scale have been  
405 previously investigated (Cossarini et al., 2019) and additional improvements could be provided by a 3D varying correlation radius (Storto et al., 2014).

Looking at the recent evolution in the availability of BGC-Argo sensors (Figure 13), our combined NN and DA approach would allow keeping the benefits of the BGC-Argo OS in the Mediterranean operational system. Even if nitrate and chlorophyll profiles have dramatically decreased after 2020, the assimilation of reconstructed profiles can potentially overcome this lack.  
410 Nevertheless, as shown in our OSE experiments (Figure 11 and 12), there are still undersampled areas by the Argo and oxygen sensors, such as Alboran, Southern Ionian seas and the marginal seas (Northern Adriatic and Northern Aegean Sea) which would require specific deployments.

With respect to previous BGC OSSE experiments (Yu et al. 2018, Ford 2021), we show how to exploit the current Argo and BGC-Argo networks for reconstructing biogeochemical variables.

415 MLP feed-forward methods to reconstruct biogeochemical variables are good enough (Bittig et al. 2018c, Sauzède et al. 2020, Fourier et al. 2021 and Pietropolli et al. 2023) to reach our purposes, even if their application to generate smooth and consistent profiles still has some limitations (Pietropolli et al., 2023). The MLP-NN-MED method has a validation error of  $0.50 \text{ mmol}^2 \text{ m}^{-3}$  for nitrate and  $0.87 \text{ mmol}^2 \text{ m}^{-3}$  when it is used to predict BGC-Argo data (Pietropolli et al., 2023). These values are slightly higher than the BGC-Argo error estimated from the triple collocation method (Mignot et al., 2019), which  
420 is used as the observation error. We recognized that different error values can be used for BGC-Argo and reconstructed profiles to take account of their uncertainties. Then, it is intuitive that with higher error, the reconstructed dataset impact would have been lower.

Indeed, the larger error in MLP-NN-MED prediction of BGC-Argo profiles derives the fact that the MLP methods, being pointwise based, are unaware of the vertical gradient (e.g., typical shape) of the profiles of biogeochemical variables that they  
425 seek to infer. This fact can lead to irregularities and lack of smoothness in the predicted profiles (Pietropolli et al., 2023), which we partly solved by adding a smoothing operator. However, one way to increase the reliability of profile reconstruction would be to include information with a physical meaning from observed data (Buizza et al., 2022). 1D Convolutional Neural Networks represent a viable alternative approach considering their ability to treat the coherence of the 1D signals (e.g., typical shapes of profiles) as shown in Li et al. (2021).

430 Integration of NN and DA have been tested in several geoscience applications (Buizza et al. 2022, Brajard et al. 2021, Stanev et al. 2022) to infer unresolved spatial scales or reproduce missing data. In our application, the integration of NN, which retrieves a large number of profiles (Pietropolli et al., 2023), and DA, which can apply the correction to all nutrients through error covariances (Teruzzi et al., 2021), allows spatial and multivariate changes to be captured both at the local scale and across the basin to constrain Mediterranean productivity (Figure 10). Although the corrections take time to extend to the



435 entire basin (Figure 7), our simulations have shown that constraining bottom-up ecosystem processes (e.g., productivity, organic matter sink) has proven effective and should be used in conjunction with the classical ocean color correction to phytoplankton biomass.

Any plan to learn directly from observations will have to face with some challenges, such as the use of observations whose time and space coverage is uneven or related to specific processes (Geer, 2021). The modular approach followed in this work  
440 represents a successful example of exploiting the strengths of neural networks and data assimilation to enhance the observing system impact in the operational biogeochemical system of the Mediterranean Sea.

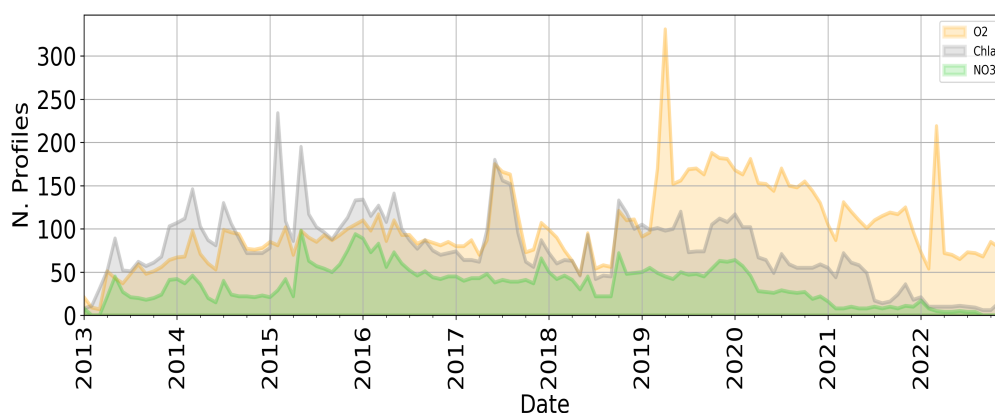


**Figure 13.** Timeserie of BGC-Argo profiles availability (2013-2022) for: nitrate (green), chlorophyll (grey) and oxygen (yellow)

## 5 Conclusions

Combining deterministic Feed-Forward Neural Network and Data Assimilation to design an Observing System Experiment has enabled demonstrating the enhanced positive impact of profiles assimilation in the Copernicus Operational System for  
445 Short-Term Forecasting of the Biogeochemistry of the Mediterranean Sea (MedBFM).

The development of the oxygen QC procedure allowed to statistically deal with optode in-situ drift and to derive accurate reconstructed profiles of nitrate, keeping the number of assimilated observations at a much higher level despite the current negative trend in BGC-Argo availability. Achieved BGC profiles density provides valuable and additional information to complement that of ocean colour in describing phytoplankton seasonal blooms and stratification dynamics at sub-basins scale.

450 The assimilation of BGC-Argo nitrate corrects a general positive bias of the model in several Mediterranean areas, and the addition of reconstructed profiles makes the correction stronger.

Together with nitrate assimilation, the phosphate update through error covariances, sustains spatial and multivariate changes that are capable of correcting key biogeochemical processes (e.g., nitracline and deep chlorophyll maximum) and to constrain ecosystem processes (e.g., productivity) at basin-wide scale.



455 *Author contributions.* CA, AT and GCoss conceived the study. CA and AT updated the 3DVarBio code and GP and LM developed the MLP-  
NN-MED model. CA and GCoi performed the simulations. CA, AT and GCoss conducted the analysis of the simulation results. CA, AT, GP  
and GCoss wrote the draft. All authors have approved the manuscript and agree with its submission.

*Competing interests.* The contact author has declared that neither they nor their co-authors have any competing interests.

*Disclaimer.* Publisher's note: Copernicus Publications remains neutral with regard to jurisdictional claims in published maps and institutional  
460 affiliations.

*Acknowledgements.* This research has been partly supported by the MED-MFC "Mediterranean Monitoring and Forecasting Centre" of  
Copernicus Marine Service, which is implemented by Mercator Ocean International within the framework of a delegation agreement with  
the European Union. (Ref. n. 21002L5-COP-MFC MED-5500).



## References

- 465 Argo: Argo float data and metadata from Global Data Assembly Centre (Argo GDAC), <https://doi.org/10.17882/42182>, 2023.
- Barbieux, M., Uitz, J., Gentili, B., Pasqueron de Fommervault, O., Mignot, A., Poteau, A., Schmechtig, C., Taillandier, V., Leymarie, E., Penkerch, C., et al.: Bio-optical characterization of subsurface chlorophyll maxima in the Mediterranean Sea from a Biogeochemical-Argo float database, *Biogeosciences*, 16, 1321–1342, 2019.
- Barbieux, M., Uitz, J., Mignot, A., Roesler, C., Claustre, H., Gentili, B., Taillandier, V., d’Ortenzio, F., Loisel, H., Poteau, A., et al.: Biological  
470 production in two contrasted regions of the Mediterranean Sea during the oligotrophic period: an estimate based on the diel cycle of optical properties measured by BioGeoChemical-Argo profiling floats, *Biogeosciences*, 19, 1165–1194, 2022.
- Bittig, H. C., Körtzinger, A., Neill, C., Van Ooijen, E., Plant, J. N., Hahn, J., Johnson, K. S., Yang, B., and Emerson, S. R.: Oxygen optode sensors: principle, characterization, calibration, and application in the ocean, *Frontiers in Marine Science*, 4, 429, 2018a.
- Bittig, H. C., Körtzinger, A., Neill, C., Van Ooijen, E., Plant, J. N., Hahn, J., Johnson, K. S., Yang, B., and Emerson, S. R.: Oxygen optode  
475 sensors: principle, characterization, calibration, and application in the ocean, *Frontiers in Marine Science*, 4, 429, 2018b.
- Bittig, H. C., Steinhoff, T., Claustre, H., Fiedler, B., Williams, N. L., Sauzède, R., Körtzinger, A., and Gattuso, J.-P.: An alternative to static climatologies: Robust estimation of open ocean CO<sub>2</sub> variables and nutrient concentrations from T, S, and O<sub>2</sub> data using Bayesian neural networks, *Frontiers in Marine Science*, 5, 328, 2018c.
- Brajard, J., Carrassi, A., Bocquet, M., and Bertino, L.: Combining data assimilation and machine learning to infer unresolved scale  
480 parametrization, *Philosophical Transactions of the Royal Society A*, 379, 20200086, 2021.
- Buga, L., Sarbu, G., Fryberg, L., Magnus, W., Wesslander, K., Gatti, J., Leroy, D., Iona, S., Larsen, M., Koefoed Rømer, J., et al.: EMODnet Thematic Lot no 4/SI2. 749773 EMODnet Chemistry Eutrophication and Acidity aggregated datasets v2018, EMODnet [data set], 2018.
- Buizza, C., Casas, C. Q., Nadler, P., Mack, J., Marrone, S., Titus, Z., Le Cornec, C., Heylen, E., Dur, T., Ruiz, L. B., et al.: Data learning: integrating data assimilation and machine learning, *Journal of Computational Science*, 58, 101–125, 2022.
- 485 Bushinsky, S. M., Emerson, S. R., Riser, S. C., and Swift, D. D.: Accurate oxygen measurements on modified Argo floats using in situ air calibrations, *Limnology and Oceanography: Methods*, 14, 491–505, 2016.
- Canu, D. M., Ghermandi, A., Nunes, P. A., Lazzari, P., Cossarini, G., and Solidoro, C.: Estimating the value of carbon sequestration ecosystem services in the Mediterranean Sea: An ecological economics approach, *Global Environmental Change*, 32, 87–95, 2015.
- Capet, A., Stanev, E. V., Beckers, J.-M., Murray, J. W., and Grégoire, M.: Decline of the Black Sea oxygen inventory, *Biogeosciences*, 13,  
490 1287–1297, 2016.
- Coppini, G., Clementi, E., Cossarini, G., Salon, S., Korres, G., Ravdas, M., Lecci, R., Pistoia, J., Goglio, A. C., Drudi, M., et al.: The Mediterranean forecasting system. Part I: evolution and performance, *EGUsphere*, pp. 1–50, 2023.
- Coppola, L., Legendre, L., Lefevre, D., Prieur, L., Taillandier, V., and Riquier, E. D.: Seasonal and inter-annual variations of dissolved oxygen in the northwestern Mediterranean Sea (DYFAMED site), *Progress in Oceanography*, 162, 187–201, 2018.
- 495 Cossarini, G., Lazzari, P., and Solidoro, C.: Spatiotemporal variability of alkalinity in the Mediterranean Sea, *Biogeosciences*, 12, 1647–1658, 2015a.
- Cossarini, G., Querin, S., and Solidoro, C.: The continental shelf carbon pump in the northern Adriatic Sea (Mediterranean Sea): Influence of wintertime variability, *Ecological Modelling*, 314, 118–134, 2015b.



- Cossarini, G., Mariotti, L., Feudale, L., Mignot, A., Salon, S., Taillandier, V., Teruzzi, A., and d'Ortenzio, F.: Towards operational 3D-Var  
500 assimilation of chlorophyll Biogeochemical-Argo float data into a biogeochemical model of the Mediterranean Sea, *Ocean Modelling*,  
133, 112–128, 2019.
- Cossarini, G., Feudale, L., Teruzzi, A., Bolzon, G., Coidessa, G., Solidoro, C., Di Biagio, V., Amadio, C., Lazzari, P., Brosich, A., et al.:  
High-Resolution Reanalysis of the Mediterranean Sea Biogeochemistry (1999–2019), *Frontiers in Marine Science*, 8, 741 486, 2021.
- Dall'Olmo, G. and Mork, K. A.: Carbon export by small particles in the Norwegian Sea, *Geophysical Research Letters*, 41, 2921–2927,  
505 2014.
- Dang, X., Peng, H., Wang, X., and Zhang, H.: Theil-sen estimators in a multiple linear regression model, *Olemiss Edu*, 2008.
- Di Biagio, V., Salon, S., Feudale, L., and Cossarini, G.: Subsurface oxygen maximum in oligotrophic marine ecosystems: mapping the  
interaction between physical and biogeochemical processes, *Biogeosciences Discussions*, pp. 1–33, 2022.
- Dobricic, S., Pinardi, N., Adani, M., Tonani, M., Fratianni, C., Bonazzi, A., and Fernandez, V.: Daily oceanographic analyses by the Mediter-  
510 ranean basin scale assimilation system, *Ocean Science Discussions*, 3, 1977–1998, 2006.
- d'Ortenzio, F., Taillandier, V., Claustre, H., Coppola, L., Conan, P., Dumas, F., Durrieu du Madron, X., Fourier, M., Gogou, A., Karageorgis,  
A., et al.: BGC-Argo floats observe nitrate injection and spring phytoplankton increase in the surface layer of Levantine Sea (Eastern  
Mediterranean), *Geophysical Research Letters*, 48, e2020GL091 649, 2021.
- D'ortenzio, F., Taillandier, V., Claustre, H., Prieur, L. M., Leymarie, E., Mignot, A., Poteau, A., Penker'h, C., and Schmechtig, C. M.:  
515 Biogeochemical Argo: The test case of the NAOS Mediterranean array, *Frontiers in Marine Science*, 7, 120, 2020.
- Escudier, R., Clementi, E., Cipollone, A., Pistoia, J., Drudi, M., Grandi, A., Lyubartsev, V., Lecci, R., Aydogdu, A., Delrosso, D., et al.: A  
high resolution reanalysis for the Mediterranean Sea, *Frontiers in Earth Science*, p. 1060, 2021.
- Fennel, K., Gehlen, M., Brasseur, P., Brown, C. W., Ciavatta, S., Cossarini, G., Crise, A., Edwards, C. A., Ford, D., Friedrichs, M. A.,  
et al.: Advancing marine biogeochemical and ecosystem reanalyses and forecasts as tools for monitoring and managing ecosystem health,  
520 *Frontiers in Marine Science*, 6, 89, 2019.
- Fischler, M. A. and Bolles, R. C.: Random sample consensus: a paradigm for model fitting with applications to image analysis and automated  
cartography, *Communications of the ACM*, 24, 381–395, 1981.
- Ford, D.: Assimilating synthetic Biogeochemical-Argo and ocean colour observations into a global ocean model to inform observing system  
design, *Biogeosciences*, 18, 509–534, 2021.
- 525 Foujols, M.-A., Lévy, M., Aumont, O., and Madec, G.: OPA 8.1 Tracer model reference manual, Institut Pierre Simon Laplace, p. 39, 2000.
- Fourrier, M., Coppola, L., Claustre, H., D'Ortenzio, F., Sauzède, R., and Gattuso, J.-P.: A regional neural network approach to estimate  
water-column nutrient concentrations and carbonate system variables in the Mediterranean Sea: CANYON-MED, *Frontiers in Marine  
Science*, 7, 620, 2020.
- Fourrier, M., Coppola, L., Claustre, H., D'Ortenzio, F., Sauzède, R., and Gattuso, J.-P.: Corrigendum: A regional neural network approach  
530 to estimate water-column nutrient concentrations and carbonate system variables in the Mediterranean Sea: CANYON-MED, *Frontiers in  
Marine Science*, 8, 650 509, 2021.
- Gasparin, F., Guinehut, S., Mao, C., Mirouze, I., Rémy, E., King, R. R., Hamon, M., Reid, R., Storto, A., Le Traon, P.-Y., et al.: Requirements  
for an integrated in situ Atlantic Ocean observing system from coordinated observing system simulation experiments, *Frontiers in Marine  
Science*, 6, 83, 2019.
- 535 Geer, A.: Learning earth system models from observations: machine learning or data assimilation?, *Philosophical Transactions of the Royal  
Society A*, 379, 20200 089, 2021.





- Hornik, K., Stinchcombe, M., and White, H.: Multilayer feedforward networks are universal approximators, *Neural networks*, 2, 359–366, 1989.
- Johnson, K. and Claustre, H.: Bringing biogeochemistry into the Argo age, *Eos, Transactions American Geophysical Union*, 2016.
- 540 Johnson, K. S., Coletti, L. J., Jannasch, H. W., Sakamoto, C. M., Swift, D. D., and Riser, S. C.: Long-term nitrate measurements in the ocean using the In Situ Ultraviolet Spectrophotometer: sensor integration into the Apex profiling float, *Journal of Atmospheric and Oceanic Technology*, 30, 1854–1866, 2013.
- Johnson, K. S., Plant, J. N., Riser, S. C., and Gilbert, D.: Air oxygen calibration of oxygen optodes on a profiling float array, *Journal of Atmospheric and Oceanic Technology*, 32, 2160–2172, 2015.
- 545 Kaufman, D. E., Friedrichs, M. A., Hemmings, J. C., and Smith Jr, W. O.: Assimilating bio-optical glider data during a phytoplankton bloom in the southern Ross Sea, *Biogeosciences*, 15, 73–90, 2018.
- Kumar, S., Peters-Lidard, C., Santanello, J., Reichle, R., Draper, C., Koster, R., Nearing, G., and Jasinski, M.: Evaluating the utility of satellite soil moisture retrievals over irrigated areas and the ability of land data assimilation methods to correct for unmodeled processes, *Hydrology and Earth System Sciences*, 19, 4463–4478, 2015.
- 550 Lary, D. J., Zewdie, G. K., Liu, X., Wu, D., Levetin, E., Allee, R. J., Malakar, N., Walker, A., Mussa, H., Mannino, A., et al.: Machine learning applications for earth observation, *Earth observation open science and innovation*, 165, 2018.
- Lazzari, P., Solidoro, C., Ibello, V., Salon, S., Teruzzi, A., Béranger, K., Colella, S., and Crise, A.: Seasonal and inter-annual variability of plankton chlorophyll and primary production in the Mediterranean Sea: a modelling approach, *Biogeosciences*, 9, 217–233, 2012.
- Lazzari, P., Solidoro, C., Salon, S., and Bolzon, G.: Spatial variability of phosphate and nitrate in the Mediterranean Sea: A modeling approach, *Deep Sea Research Part I: Oceanographic Research Papers*, 108, 39–52, 2016.
- 555 Le Traon, P.-Y.: From satellite altimetry to Argo and operational oceanography: three revolutions in oceanography, *Ocean Science*, 9, 901–915, 2013.
- Le Traon, P. Y., Reppucci, A., Alvarez Fanjul, E., Aouf, L., Behrens, A., Belmonte, M., Bentamy, A., Bertino, L., Brando, V. E., Kreiner, M. B., et al.: From observation to information and users: The Copernicus Marine Service perspective, *Frontiers in Marine Science*, 6, 234, 2019.
- 560 Li, Z., Liu, F., Yang, W., Peng, S., and Zhou, J.: A survey of convolutional neural networks: analysis, applications, and prospects, *IEEE transactions on neural networks and learning systems*, 2021.
- Li, Z. Q., Liu, Z. H., and Lu, S. L.: Global Argo data fast receiving and post-quality-control system, *IOP Conference Series: Earth and Environmental Science*, 502, 012 012, <https://doi.org/10.1088/1755-1315/502/1/012012>, 2020.
- 565 Mancini, A. M., Bocci, G., Morigi, C., Gennari, R., Lozar, F., and Negri, A.: Past Analogues of Deoxygenation Events in the Mediterranean Sea: A Tool to Constrain Future Impacts, *Journal of Marine Science and Engineering*, 11, 562, 2023.
- Marañón, E., Van Wambeke, F., Uitz, J., Boss, E. S., Dimier, C., Dinasquet, J., Engel, A., Haëntjens, N., Pérez-Lorenzo, M., Taillandier, V., et al.: Deep maxima of phytoplankton biomass, primary production and bacterial production in the Mediterranean Sea, *Biogeosciences*, 18, 1749–1767, 2021.
- 570 Martínez, E., Brini, A., Gorgues, T., Drumetz, L., Roussillon, J., Tandeo, P., Maze, G., and Fablet, R.: Neural network approaches to reconstruct phytoplankton time-series in the global ocean, *Remote Sensing*, 12, 4156, 2020a.
- Martínez, E., Gorgues, T., Lengaigne, M., Fontana, C., Sauzède, R., Menkes, C., Uitz, J., Di Lorenzo, E., and Fablet, R.: Reconstructing global chlorophyll-a variations using a non-linear statistical approach, *Frontiers in Marine Science*, 7, 464, 2020b.



- Maurer, T. L., Plant, J. N., and Johnson, K. S.: Delayed-mode quality control of oxygen, nitrate, and pH data on SOCCOM biogeochemical profiling floats, *Frontiers in Marine Science*, 8, 683–207, 2021.
- 575
- Mavropoulou, A.-M., Vervatis, V., and Sofianos, S.: Dissolved oxygen variability in the Mediterranean Sea, *Journal of Marine Systems*, 208, 103–348, 2020.
- Mignot, A., Claustre, H., Uitz, J., Poteau, A., d’Ortenzio, F., and Xing, X.: Understanding the seasonal dynamics of phytoplankton biomass and the deep chlorophyll maximum in oligotrophic environments: A Bio-Argo float investigation, *Global Biogeochemical Cycles*, 28, 856–876, 2014.
- 580
- Mignot, A., d’Ortenzio, F., Taillandier, V., Cossarini, G., and Salon, S.: Quantifying observational errors in Biogeochemical-Argo oxygen, nitrate, and chlorophyll a concentrations, *Geophysical Research Letters*, 46, 4330–4337, 2019.
- Miloslavich, P., Seeyave, S., Muller-Karger, F., Bax, N., Ali, E., Delgado, C., Evers-King, H., Loveday, B., Lutz, V., Newton, J., et al.: Challenges for global ocean observation: the need for increased human capacity, *Journal of Operational Oceanography*, 12, S137–S156, 2019.
- 585
- Oddo, P., Adani, M., Pinardi, N., Fratianni, C., Tonani, M., and Pettenuzzo, D.: A nested Atlantic-Mediterranean Sea general circulation model for operational forecasting, *Ocean science*, 5, 461–473, 2009.
- Pietropolli, G., Manzoni, L., and Cossarini, G.: Multivariate Relationship in Big Data Collection of Ocean Observing System, *Applied Sciences*, 13, 5634, 2023.
- 590
- Pinardi, N., Zavatarelli, M., Adani, M., Coppini, G., Fratianni, C., Oddo, P., Simoncelli, S., Tonani, M., Lyubartsev, V., Dobricic, S., et al.: Mediterranean Sea large-scale low-frequency ocean variability and water mass formation rates from 1987 to 2007: A retrospective analysis, *Progress in Oceanography*, 132, 318–332, 2015.
- Raichich, F. and Rampazzo, A.: Observing System Simulation Experiments for the assessment of temperature sampling strategies in the Mediterranean Sea, *Annales Geophysicae*, 21, 151–165, <https://doi.org/10.5194/angeo-21-151-2003>, 2003.
- 595
- Ricour, F., Capet, A., d’Ortenzio, F., Delille, B., and Grégoire, M.: Dynamics of the deep chlorophyll maximum in the Black Sea as depicted by BGC-Argo floats, *Biogeosciences*, 18, 755–774, 2021.
- Roussillon, J., Fablet, R., Gorgues, T., Drumetz, L., Littaye, J., and Martinez, E.: A Multi-Mode Convolutional Neural Network to reconstruct satellite-derived chlorophyll-a time series in the global ocean from physical drivers, *Frontiers in Marine Science*, 10, 2023.
- Salon, S., Cossarini, G., Bolzon, G., Feudale, L., Lazzari, P., Teruzzi, A., Solidoro, C., and Crise, A.: Novel metrics based on Biogeochemical Argo data to improve the model uncertainty evaluation of the CMEMS Mediterranean marine ecosystem forecasts, *Ocean Science*, 15, 997–1022, 2019.
- 600
- Sauzède, R., Claustre, H., Uitz, J., Jamet, C., Dall’Olmo, G., d’Ortenzio, F., Gentili, B., Poteau, A., and Schmechtig, C.: A neural network-based method for merging ocean color and Argo data to extend surface bio-optical properties to depth: Retrieval of the particulate backscattering coefficient, *Journal of Geophysical Research: Oceans*, 121, 2552–2571, 2016.
- 605
- Sauzède, R., Bittig, H. C., Claustre, H., Pasqueron de Fommervault, O., Gattuso, J.-P., Legendre, L., and Johnson, K. S.: Estimates of water-column nutrient concentrations and carbonate system parameters in the global ocean: a novel approach based on neural networks, *Frontiers in Marine Science*, 4, 128, 2017.
- Sauzède, R., Johnson, J., Claustre, H., Camps-Valls, G., and Ruescas, A.: Estimation of oceanic particulate organic carbon with machine learning, *ISPRS Annals of Photogrammetry, Remote Sensing and Spatial Information Sciences*, 2, 949–956, 2020.
- 610
- Siokou-Frangou, I., Christaki, U., Mazzocchi, M. G., Montesor, M., Ribera d’Alcalá, M., Vaqué, D., and Zingone, A.: Plankton in the open Mediterranean Sea: a review, *Biogeosciences*, 7, 1543–1586, 2010.



- Sisma-Ventura, G., Kress, N., Silverman, J., Gertner, Y., Ozer, T., Biton, E., Lazar, A., Gertman, I., Rahav, E., and Herut, B.: Post-eastern mediterranean transient oxygen decline in the deep waters of the southeast mediterranean sea supports weakening of ventilation rates, *Frontiers in Marine Science*, 7, 598 686, 2021.
- 615 Skakala, J., Ford, D., Bruggeman, J., Hull, T., Kaiser, J., King, R. R., Loveday, B., Palmer, M. R., Smyth, T., Williams, C. A., et al.: Towards a multi-platform assimilative system for North Sea biogeochemistry, *Journal of Geophysical Research: Oceans*, 126, e2020JC016 649, 2021.
- Stanev, E. V., Wahle, K., and Staneva, J.: The synergy of data from profiling floats, machine learning and numerical modeling: Case of the Black Sea euphotic zone, *Journal of Geophysical Research: Oceans*, 127, e2021JC018 012, 2022.
- 620 Storto, A., Masina, S., and Dobricic, S.: Estimation and impact of nonuniform horizontal correlation length scales for global ocean physical analyses, *Journal of Atmospheric and Oceanic Technology*, 31, 2330–2349, 2014.
- Storto, A., De Magistris, G., Falchetti, S., and Oddo, P.: A neural network–based observation operator for coupled ocean–acoustic variational data assimilation, *Monthly Weather Review*, 149, 1967–1985, 2021.
- Taillandier, V., Prieur, L., d’Ortenzio, F., Ribera d’Alcalà, M., and Pulido-Villena, E.: Profiling float observation of thermohaline staircases 625 in the western Mediterranean Sea and impact on nutrient fluxes, *Biogeosciences*, 17, 3343–3366, 2020.
- Takeshita, Y., Martz, T. R., Johnson, K. S., Plant, J. N., Gilbert, D., Riser, S. C., Neill, C., and Tilbrook, B.: A climatology-based quality control procedure for profiling float oxygen data, *Journal of Geophysical Research: Oceans*, 118, 5640–5650, 2013.
- Teruzzi, A., Dobricic, S., Solidoro, C., and Cossarini, G.: A 3-D variational assimilation scheme in coupled transport-biogeochemical models: Forecast of Mediterranean biogeochemical properties, *Journal of Geophysical Research: Oceans*, 119, 200–217, 2014.
- 630 Teruzzi, A., Bolzon, G., Salon, S., Lazzari, P., Solidoro, C., and Cossarini, G.: Assimilation of coastal and open sea biogeochemical data to improve phytoplankton simulation in the Mediterranean Sea, *Ocean Modelling*, 132, 46–60, 2018.
- Teruzzi, A., Bolzon, G., Feudale, L., and Cossarini, G.: Deep chlorophyll maximum and nutricline in the Mediterranean Sea: emerging properties from a multi-platform assimilated biogeochemical model experiment, *Biogeosciences*, 18, 6147–6166, 2021.
- Terzić, E., Lazzari, P., Organelli, E., Solidoro, C., Salon, S., d’Ortenzio, F., and Conan, P.: Merging bio-optical data from Biogeochemical- 635 Argo floats and models in marine biogeochemistry, *Biogeosciences*, 16, 2527–2542, 2019.
- Thierry, V. and Bittig, H.: Argo quality control manual for dissolved oxygen concentration, Report (qualification paper (procedure, accreditation support)), FRANCE, <https://doi.org/https://doi.org/10.13155/46542>, 2021.
- Verdy, A. and Mazloff, M. R.: A data assimilating model for estimating Southern Ocean biogeochemistry, *Journal of Geophysical Research: Oceans*, 122, 6968–6988, 2017.
- 640 Vichi, M., Pinardi, N., and Masina, S.: A generalized model of pelagic biogeochemistry for the global ocean ecosystem. Part I: Theory, *Journal of Marine Systems*, 64, 89–109, 2007a.
- Vichi, M., Pinardi, N., and Masina, S.: A generalized model of pelagic biogeochemistry for the global ocean ecosystem. Part I: Theory, *Journal of Marine Systems*, 64, 89–109, 2007b.
- Wang, B. and Fennel, K.: An assessment of vertical carbon flux parameterizations using backscatter data from BGC Argo, *Geophysical Research Letters*, 50, e2022GL101 220, 2023.
- 645 Wang, B., Fennel, K., Yu, L., and Gordon, C.: Assessing the value of biogeochemical Argo profiles versus ocean color observations for biogeochemical model optimization in the Gulf of Mexico, *Biogeosciences*, 17, 4059–4074, 2020.
- Wang, B., Fennel, K., and Yu, L.: Can assimilation of satellite observations improve subsurface biological properties in a numerical model? A case study for the Gulf of Mexico, *Ocean Science*, 17, 1141–1156, 2021a.



- 650 Wang, S., Flipo, N., Romary, T., and Hasanyar, M.: Particle filter for high frequency oxygen data assimilation in river systems, *Environmental Modelling & Software*, 151, 105 382, 2022.
- Wang, T., Chai, F., Xing, X., Ning, J., Jiang, W., and Riser, S. C.: Influence of multi-scale dynamics on the vertical nitrate distribution around the Kuroshio Extension: An investigation based on BGC-Argo and satellite data, *Progress In Oceanography*, 193, 102 543, 2021b.
- Yu, L., Fennel, K., Bertino, L., El Gharamti, M., and Thompson, K. R.: Insights on multivariate updates of physical and biogeochemical  
655 ocean variables using an Ensemble Kalman Filter and an idealized model of upwelling, *Ocean Modelling*, 126, 13–28, 2018.
- Zhou, H., Yue, X., Lei, Y., Tian, C., Ma, Y., and Cao, Y.: Large contributions of diffuse radiation to global gross primary productivity during 1981–2015, *Global Biogeochemical Cycles*, 35, e2021GB006 957, 2021.